
Article:
Meng, X, Zhang, Z-Q orcid.org/0000-0003-0204-3867, Wu, J-K et al. (2 more authors) (2014) Self-Contained Pedestrian Tracking During Normal Walking Using an Inertial/Magnetic Sensor Module. IEEE Transactions on Biomedical Engineering, 61 (3). pp. 892-899. ISSN 0018-9294

https://doi.org/10.1109/TBME.2013.2291910

Self-contained Pedestrian Tracking during Normal Walking using an Inertial/Magnetic Sensor Module

Xiaoli Meng, Zhi-Qiang Zhang*, Jian-Kang Wu, Wai-Choong Wong, and Haoyong Yu

***Abstract*—This paper proposes a novel self-contained pedestrian tracking method using a foot-mounted inertial and magnetic sensor module, which not only uses the traditional zero velocity updates (ZUPT), but also applies the stride information to further correct the acceleration double integration drifts and thus improves the tracking accuracy. In our method, a velocity control variable is designed in the process model, which is set to the average velocity derived from stride information in the swing (non-zero velocity) phases or zero in the stance (zero-velocity) phases. Stride-based position information is also derived as the pseudo-measurements to further improve the accuracy of the position estimates. An adaptive Kalman filter (AKF) is then designed to fuse all the sensor information and pseudo-measurements. The proposed pedestrian tracking method has been extensively evaluated using experiments, including both short distance walking with different patterns and long distance walking performed indoors and outdoors, and have been shown to perform effectively for pedestrian tracking.**

***Index Terms*—Sensor fusion, zero velocity update, stride counting, Unscented Kalman filter, pedestrian navigation.**

I. Introduction

SELF-CONTAINED pedestrian navigation systems have been applied in numerous applications, such as rescue/emergency first response, location-aware computing, augmented reality and so on [1]. Until now, current outdoor position tracking technologies mainly rely on GPS, which normally requires an unobstructed line of sight to four or more GPS satellites [2]. However, in urban and indoor environments GPS signals are unreliable or even unavailable due to the signal attenuation caused by buildings, tunnels, and other construction materials. Various acoustic, optical or radio frequency (RF) localization systems have been suggested so far, but such systems all require complicated setup and calibration, which impose tremendous challenges for routine use [3].

As wearable sensors can work in arbitrary unprepared indoor and outdoor environments, to this end, self-contained pedestrian tracking systems based on inertial/magnetic measurement units have attracted lots of research interests. A typical inertial/magnetic measurement unit contains a triaxial accelerometer, a triaxial angular rate sensor, and a triaxial magnetometer, and these sensor units are already commercially available on the market at reasonable cost [4] [5]. The basic idea of the inertial/magnetic measurement unit-based pedestrian tracking is an adaptation of the well-known strapdown navigation algorithm, which incorporates double integration of the measured acceleration to estimate distance or position. However, it is extremely difficult to extract accurate motion accelerations from the accelerometer signals due to sensor bias and noises, and any small error can make the position error increase exponentially; therefore, zero-velocity updates (ZUPTs) are commonly employed to mitigate this problem by resetting the accumulated error [6] [7]. This technique exploits the intrinsic property of pedestrian walking: there are repeated recognizable periods when the foot stays stationary on the ground, during which the velocity and acceleration of the foot are zero. Extensive research has been performed on how to use ZUPTs for accurate position estimation. For example, both Ojeda *et al.* [8] and Bebek *et al.* [9] simply reset the integrated velocity to zero during the zero velocity phases. Foxlin [10] and Godha *et al.* [11] introduced ZUPTs as pseudo-measurements into an extended Kalman filter as the navigation error corrector. Instead of simply resetting the accumulated velocity error periodically, Yun *et al.* [12] further improved the idea of ZUPTs and applied a time variant acceleration bias error to revise the acceleration in the swing phases. Although the removal of the acceleration bias error can significantly improve the accuracy of position tracking, it is still problematic for long distance tracking.

To increase the accuracy of the ZUPT-based methods over long durations, some extra infrastructures and technologies, such as ultrasound, short-range radio (Wi-Fi, Ultra-Wideband (UWB), radio frequency identification (RFID) and Zigbee) or vision, have been explored in pedestrian navigation together with the inertial/magnetic sensor units. For instance, Fischer *et al.* [13] proposed a pedestrian navigation system based on a combination of foot-mounted inertial sensors and ultrasound beacons. Both Hol *et al.* [14] and Corrales *et al.* [15] combined UWB with inertial/magnetic sensor units for position tracking. Ruiz *et al.* [16] fused inertial navigation system (INS) techniques with active RFID technology for accurate indoor pedestrian localization and navigation. Widyawana *et al.* [17] presented a multi-modal indoor navigation technique that integrated inertial/magnetic sensor units with RF and ultrasound beacons to reduce the impact of incremental er-

Manuscript received August 15, 2013; revised September 23, 2013; accepted November 15, 2013. This research is funded by National Natural Science Foundation of China (Grant No.60932001). *Asterisk indicates corresponding author.*

X. L. Meng, and H.Y. Yu are with the Department of Bioengineering, National University of Singapore, Singapore.

Z.-Q. Zhang is with the Department of Computing, Imperial College London, SW7 2AZ London, U. K. (e-mail: z.zhang@imperial.ac.uk).

J.-K. Wu is with the school of Information Science and Engineering, Graduate University of Chinese Academy of Sciences, Beijing, China, 100049.

W.-C. Wong is with the Department of Electrical and Computer Engineering, National University of Singapore, Singapore 117576.

ror accumulation. All the above mentioned methods have illustrated that the incorporation of extra infrastructures can improve location accuracy, but the extra instrumentations can make the systems less ubiquitous in terms of installation and maintenance.

However, except for ZUPT, more information, such as stride frequency, stride length and heading direction, can also be derived from the raw sensor measurements, and this information can be used for pedestrian localization as well [18] [19]. Through the counting of strides, the position of the pedestrians can be estimated based on an approximate stride length and heading direction, which can avoid the excessive double integration drifts, but is susceptible to stride mis-detection/false-detection and the errors in stride length estimation and heading direction. Moreover, the stride-based method can only be implemented with relatively low frequency to update the positions once per gait cycle.

In this paper, we propose a novel pedestrian navigation method which integrates the ZUPT-based method with the stride-based method under the framework of an adaptive Kalman filter (AKF). In order to compensate for the velocity drift, a velocity control variable is designed in the process model, which is set to the average velocity derived from the stride information in the swing (non-zero velocity) phases or zero in the stance (zero velocity) phases. Stride-based position estimates are also derived as the pseudo-measurements to further improve tracking accuracy. The proposed pedestrian tracking method has been extensively evaluated using experiments including both short distance walking with different patterns and long distance walking performed indoors and outdoors. The significant improvement of tracking accuracy in comparison with the two pure ZUPT-based methods has shown the proposed algorithm works effectively for pedestrian tracking.

The rest of the paper is organized as follows. Section II presents the proposed pedestrian tracking method under the framework of the AKF, including the stance phase detection, process model, sensor measurement model, pseudo-measurement model and adaptive filtering. Experimental results and discussions are described in Section III. Finally, we conclude the paper in Section IV.

II. Proposed Pedestrian Tracking Method

For a pedestrian navigation system, three coordinate systems are defined: 1) the global coordinate system (GCS): North east down (NED) coordinate system is introduced as the GCS with X-axis pointing north, Y-axis pointing east, and Z-axis pointing down to construct a right-handed coordinate system; 2) body coordinate system (BCS): coordinate system of the foot segment; 3) sensor coordinate system (SCS): three orthogonally axes of the mounted sensors. To facilitate our analysis, the BCS is assumed to coincide with the SCS after sensor to body alignment calibration [20].

As shown in Fig. 1, the proposed pedestrian tracking method consists of stance phase detection, process model, sensor measurement model, pseudo measurement model and adaptive filtering. We will introduce them in sequence in this section.

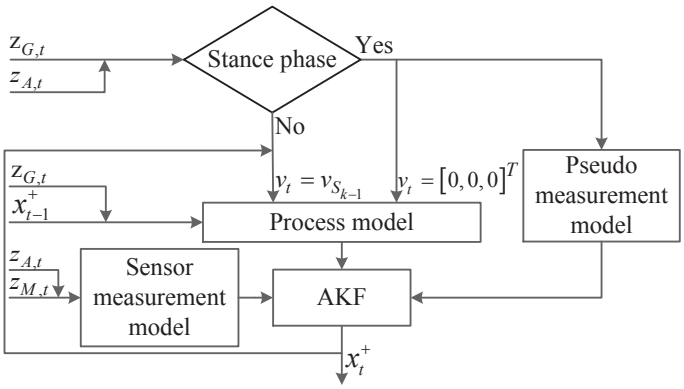

Fig. 1. The flowchart of the proposed pedestrian tracking algorithm.

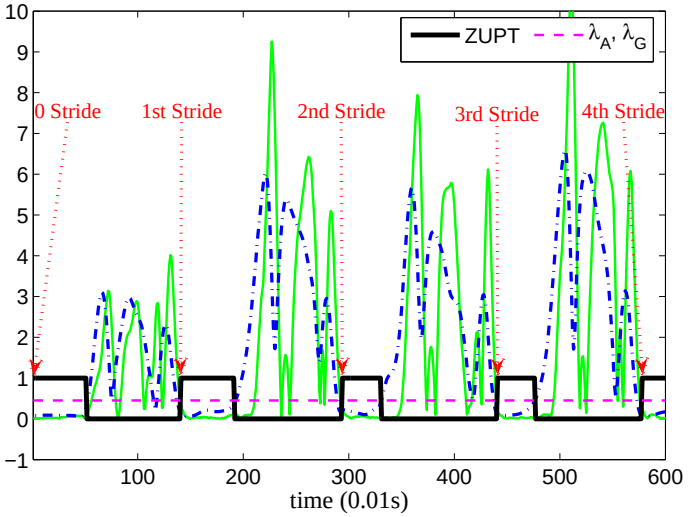

Fig. 2. The detection results of the stance phase. Green line: $\left|\|z_{A,t}\| - g\right|$; blue dash-dotted line: $\|z_{G,t}\|$; red dotted arrows: stride indices. λ_A and λ_G are set to the same value.

A. Stance Phase Detection

During any stance phase, the foot stays stationary on the ground, which means that the accelerometer only measures the gravity and the gyroscope readings should be zero. As shown in Fig. 2, a simple stance phase detector can be designed as:

$$\text{Stance} = \begin{cases} 1, & \left|\|z_{A,t}\| - g\right| < \lambda_A \text{ and } \|z_{G,t}\| < \lambda_G \\ 0, & \text{else} \end{cases} \quad (1)$$

where $z_{A,t}$ is the accelerometer measurement at time t, while the $z_{G,t}$ is the gyroscope reading at time t, $\|\cdot\|$ and $|\cdot|$ are the magnitude and absolute operations, respectively, and g denotes the gravity magnitude. λ_A and λ_G are the predefined thresholds which are set to the same value empirically in this paper.

B. Process Model

The process model employed by the AKF governs the dynamic relationship between the states of two successive time steps. The state vector at time step t, denoted by x_t, consists of position p_t, velocity v_t, motion acceleration a_t, low frequency accelerometer bias error $b_{A,t}$, and quaternion q_t associated with orientation:

$$x_t = \left[p_t^T, v_t^T, a_t^T, b_{A,t}^T, q_t^T\right]^T \quad (2)$$

where p_t, v_t, a_t and $b_{A,t}$ are defined in the GCS; q_t represents the foot's orientation relative to the GCS, and $q_t = [q_{1,t}, q_{2,t}, q_{3,t}, q_{4,t}]^T = \left[e_t^T, q_{4,t}\right]^T$, $q_{4,t}$ and $e_t = [q_{1,t},\ q_{2,t},\ q_{3,t}]^T$ are the scalar part and vector part of q_t, respectively; the superscript 'T' means 'transpose'.

The motion acceleration a_t is modeled as a first-order low-pass filtered white noise process, as in

$$a_t = c_a a_{t-1} + w_{a,t} \tag{3}$$

where c_a is a constant, and $w_{a,t}$ is a random Gaussian noise with zero mean and covariance matrix $\mathbf{Q}_a$. The slow variation of the accelerometer bias $b_{A,t}$ is modeled as a random walk driven by a Gaussian noise $w_{bA,t}$, with covariance matrix $\mathbf{Q}_{bA}$,

$$b_{A,t} = b_{A,t-1} + w_{bA,t}. \tag{4}$$

To reduce the acceleration integration drift during the swing phase, we introduce the average velocity of the last stride as an control variable in the velocity dynamic model. Thus, the velocity can be modeled as:

$$v_t = \xi\left(v_{t-1} + a_{t-1}\delta_t\right) + (1-\xi)\, v_{S_{k-1}} + w_{v,t} \tag{5}$$

where δ_t is the sampling interval (it was set to 0.01s in our implementation); $v_{S_{k-1}}$ is the average velocity of last stride calculated from stride-based tracking; k is the index of the current stride; ξ is the weight; and $w_{v,t}$ is the velocity process noise with covariance matrix $\mathbf{Q}_v$. During the stance phase, the foot velocity should be zero. To get a unified equation, the velocity in the stance phase can be written in the following form:

$$v_t = \xi\left(v_{t-1} + a_{t-1}\delta_t\right) + (1-\xi)\left[0\ \ 0\ \ 0\right]^T + w_{v,t} \tag{6}$$

where $\left[0\ \ 0\ \ 0\right]^T$ is the control vector during the stance phase and ξ is set to 0. The covariance matrix of the process noise for velocity $w_{v,t}$ in the stance phase would also be a zero matrix. In summary, the control vector u_t can be defined as follows:

$$u_t = \begin{cases} v_{S_{k-1}}, & \text{Stance} = 0 \\ \left[0\ \ 0\ \ 0\right]^T, & \text{Stance} = 1 \end{cases} \tag{7}$$

The position of the foot is calculated by

$$p_t = p_{t-1} + v_{t-1}\delta_t + \frac{1}{2}a_{t-1}\delta_t^2 + w_{p,t} \tag{8}$$

where $w_{p,t}$ is the position process noise with covariance matrix $\mathbf{Q}_p$.

Given the gyroscope measures $z_{G,t}$, the foot orientation q_t at time step t can be propagated as [21]:

$$q_t = \exp\left(\frac{1}{2}\Omega\left[z_{G,t}\right]\delta_t\right) q_{t-1} + w_{q,t} \tag{9}$$

where $\Omega\left[z_{G,t}\right]$ is a 4×4 skew symmetric matrix as in

$$\Omega\left[z_{G,t}\right] = \begin{bmatrix} -\left[z_{G,t}\times\right] & z_{G,t} \\ -z_{G,t}^T & 0 \end{bmatrix}, \tag{10}$$

$[\times]$ represents the cross product operator [22], and $w_{q,t}$ is a zero-mean Gaussian noise with covariance matrix $\mathbf{Q}_q$.

From (3)–(6), (8), and (9), the linear process model can be summarized as:

$$\begin{aligned} x_t &= \mathbf{F}_t x_{t-1} + u_t + w_t \\ &= \begin{bmatrix} \mathbf{I}_3 & \delta_t\mathbf{I}_3 & \frac{1}{2}\delta_t^2\mathbf{I}_3 & \mathbf{0}_{3\times3} & \mathbf{0}_{3\times4} \\ \mathbf{0}_{3\times3} & \xi\mathbf{I}_3 & \xi\delta_t\mathbf{I}_3 & \mathbf{0}_{3\times3} & \mathbf{0}_{3\times4} \\ \mathbf{0}_{3\times3} & \mathbf{0}_{3\times3} & c_a\mathbf{I}_3 & \mathbf{0}_{3\times3} & \mathbf{0}_{3\times4} \\ \mathbf{0}_{3\times3} & \mathbf{0}_{3\times3} & \mathbf{0}_{3\times4} & \mathbf{I}_3 & \mathbf{0}_{3\times4} \\ \mathbf{0}_{4\times3} & \mathbf{0}_{4\times3} & \mathbf{0}_{4\times3} & \mathbf{0}_{4\times3} & \mathbf{A}_t \end{bmatrix} x_{t-1} + \\ &\quad (1-\xi)\begin{bmatrix} \mathbf{0}_{3\times1} \\ u_t \\ \mathbf{0}_{3\times1} \\ \mathbf{0}_{3\times1} \\ \mathbf{0}_{3\times1} \end{bmatrix} + \begin{bmatrix} w_{p,t} \\ w_{v,t} \\ w_{a,t} \\ w_{bA,t} \\ w_{q,t} \end{bmatrix} \end{aligned} \tag{11}$$

where $\mathbf{I}_3$ denotes a 3×3 identity matrix; $\mathbf{0}$ stands for zero matrix; and $\mathbf{A}_t$ is the transition matrix given by

$$\mathbf{A}_t = \exp\left(\frac{1}{2}\mathbf{\Omega}\left[z_{G,t}\right]\delta_t\right). \tag{12}$$

In this paper, $w_{p,t}$, $w_{v,t}$, $w_{a,t}$, $w_{bA,t}$ and $w_{q,t}$ are assumed to be uncorrelated with each other, thus the process noise covariance matrix $\mathbf{Q}_t$ will have the following expression:

$$\mathbf{Q}_t = \mathrm{diag}\left(\left[\mathbf{Q}_p, \mathbf{Q}_v, \mathbf{Q}_a, \mathbf{Q}_{bA}, \mathbf{Q}_q\right]\right). \tag{13}$$

C. Sensor Measurement Model

The gravity acceleration and earth magnetic field strength are used to compensate for the predicted quaternion to get drift-free orientation estimation. Given a quaternion q_t and the reference magnetic vector in the GCS r_M, the measurement equation of the magnetometer signal $z_{M,t}$ can be defined as:

$$z_{M,t} = C(q_t)\, r_M + n_{M,t} \tag{14}$$

where $C(q_t)$ is the corresponding rotational matrix of the quaternion q_t [22]:

$$C(q_t) = \left(q_{4,t}^2 - e_t^T e_t\right)\mathbf{I}_3 + 2e_t e_t^T - 2q_{4,t}\left[e_t\times\right] \tag{15}$$

where $n_{M,t}$ is the magnetometer measurement noise with zero mean and covariance matrix $\mathbf{\Sigma}_{M,t}$. As the magnetometer measurements include the earth magnetic field and disturbance from environments, which would introduce inaccuracy to the orientation estimates. The influence from the magnetic disturbance to the orientation estimates is guarded by the adaptive mechanism proposed in [23].

The accelerometer measures gravitational acceleration together with acceleration caused by human motion, plus bias and measurement noises, as in

$$z_{A,t} = C(q_t)\left(a_t + g_0 + b_{A,t}\right) + n_{A,t} \tag{16}$$

where $n_{A,t}$ is the accelerometer measurement noise with covariance $\mathbf{\Sigma}_A$; and g_0 denotes the gravitational acceleration in GCS.

From (14) and (16), the sensor measurement model is given by:

$$\begin{aligned} z_{S,t} &= \begin{bmatrix} z_{M,t} \\ z_{A,t} \end{bmatrix} = f(x_t) + n_{S,t} \\ &= C(q_t)\cdot\begin{bmatrix} r_M \\ a_t + g_0 + b_{A,t} \end{bmatrix} + \begin{bmatrix} n_{M,t} \\ n_{A,t} \end{bmatrix} \end{aligned} \tag{17}$$

The covariance matrix of the sensor measurement noises $n_{S,t}$, denoted by $\mathbf{R}_{S,t}$, is given by:

$$\mathbf{R}_{S,t} = \begin{bmatrix} \mathbf{\Sigma}_{M,t} & \mathbf{0}_{3\times3} \\ \mathbf{0}_{3\times3} & \mathbf{\Sigma}_A \end{bmatrix} \tag{18}$$

D. Pseudo Measurement Model

The pseudo measurements of the position attained from the stride information during the stance phase can further improve tracking accuracy of the pedestrians. According to the stride-based pedestrian tracking method, at time t, when the k^{th} stride occurs, the pseudo measurements of the pedestrian location $z_{P,t}$ can be updated by:

$$z_{P,t} = l_{p,k-1} + [S_k \cos\theta_k, S_k \sin\theta_k, 0] \tag{19}$$

where $l_{p,k-1}$ is the location of the previous stride after the AKF update; S_k and θ_k are the stride length and the heading angle of the current stride, respectively. The above equation requires three important steps: stride detection, stride length estimation and heading angle determination. Here, stride detection is the same as the stance detection, so we will only introduce the stride length estimation and heading angle determination.

1) Stride length estimation: in practice, stride length varies from across different strides, but it has shown some relationship to the angular rates [24], which is given below:

$$S_k = K \cdot \sqrt[4]{Y_{G,k}^{\max} - Y_{G,k}^{\min}} \tag{20}$$

where $Y_{G,k}^{\max}$ and $Y_{G,k}^{\min}$ are the maximum and minimum values of the angular rates along the Y-axis during the k^{th} stride, respectively. The constant K is personal-dependent and determined through off-line training by collecting some walking data before the actual experiments from the subject.

2) Heading angle determination: when a stride is detected, the heading angle θ_k is extracted from the orientation of the k^{th} stride, represented by q_{S_k}, as given in:

$$\theta_k = \text{atan2}\left(2(q_{S_k,4}q_{S_k,3} + q_{S_k,1}q_{S_k,2}), 1 - 2(q_{S_k,2}^2 + q_{S_k,3}^2)\right) - \theta_0 \tag{21}$$

where θ_0 is the initial foot toe-out angle, which is assumed to be the same of each stride.

To sum up, when a stride is detected, the pseudo measurement equation is governed by:

$$z_{P,t} = p_t + n_{P,t} \tag{22}$$

where $n_{P,t}$ is zero mean Gaussian noise with covariance $\mathbf{\Sigma}_P$.

E. Adaptive Filtering Design

Through the process model (11), the measurement model (17) and (22), the ZUPT-based method is tightly integrated with the stride-based method. Because of the nonlinear measurement function (17), the Unscented Kalman Filter (UKF) is employed in this paper. The detailed UKF equations can be found in [25]. To avoid the effects of stride mis-detection/false-detection or errors in stride length estimation and the heading direction, the pseudo measurement $z_{P,t}$ is regarded as invalid and disregarded when the k^{th} stride is detected if:

$$\left| \|z_{P,t}\| - \left\|p_t^-\right\| \right| > \lambda_p, \tag{23}$$

Fig. 3. The attachment of a sensor module on the right foot of the tester.

where p_t^- is the predicted position using the process model, and λ_p is the error threshold of the position. Otherwise, the pseudo position measurement $z_{P,t}$ will be used to update the position estimates to get the location of the pedestrian at time t, denoted by p_t^+, and the control vector v_{S_k} in (5) is also updated by

$$v_{S_k} = \frac{[S_k \cos\theta_k, S_k \sin\theta_k, 0]}{T_{S_k}} \tag{24}$$

where T_{S_k} is the swing phase duration of the k^{th} stride.

III. Experimental Results

A. Experimental Setup

To evaluate the performance of the proposed algorithm, an inertial/magnetic sensor module is placed on the right foot as shown in Fig. 3. The sensor chip is the ADIS16405 from Analog Devices, which contains a triaxial accelerometer, triaxial gyroscope and triaxial magnetometer [26]. The sensor module is connected to a base station by SPI serial data bus, and it controls the data collection and send the data to PC for offline processing through Bluetooth. All the data analysis was implemented using MATLAB on a PC with 3.40 GHz Intel Core i5 processor and 8G RAM. Two types of walking experiments are carried out to validate the performance of the algorithm. Simple walking experiments including straight line walking, turning around and circle walking are evaluated first. As follows, long distance walking experiments performed both indoors and outdoors are analyzed.

B. Experimental Demonstration

A comparative study between the proposed method and two ZUPT-based methods are carried out to evaluate the pedestrian tracking performance. In what follows, 'Truth' represents the marked trajectory that the tester needs to follow; 'Our' shows the tracking results of our method, while the results using Godha's method [11] and Yun's method [12] are also shown for comparison.

1) Short distance walking: for short distance walking, three experiments are carried out according to the predefined paths: 1) the subject walks in a straight line for 15m; 2) the subject walks in a straight line for 10m, makes a 180° turn and walks back to the starting point; 3) the subject walks in a circle of radius 3m. Each experiment is repeated 5 times. One example of the estimated displacements for the three experiments are

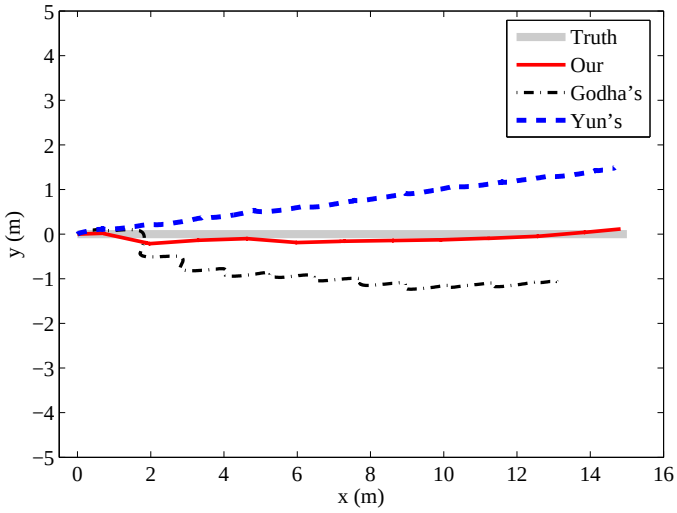

Fig. 4. One example of the estimated displacement results for walking in a straight line for 15m.

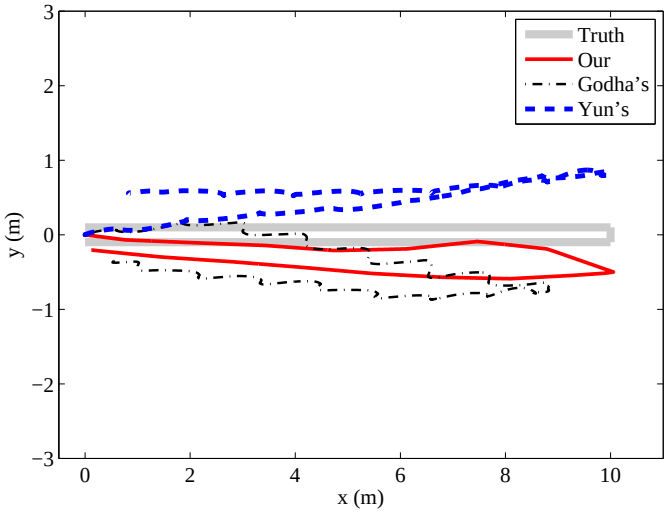

Fig. 5. One example of the estimated displacement results for walking in a straight line for 10m, and back to the starting point with a turn of 180°.

shown in Figs. 4–6, respectively. In these figures, the thick grey solid line in the plots represents the predefined path, the thin solid line shows the estimated trajectory using our proposed methods, the dotted-dashed line are the estimated results using Godha's method, and the dashed line illustrates the position estimation of Yun's method. Table I shows the position errors of each test for the three experiments. For the straight line walking, the path is not a closed-loop trajectory, and the position error is calculated using the difference between the estimated final position and the truth final position. For the other two experiments with closed-loop trajectories, the position error is evaluated by the difference between the starting and final position. Table I also show the average position errors over the 5 trials. The average position error of the proposed method for straight line walking is 0.44±0.20m, for walking with 180° turn is 0.45±0.08m, and for walking in a circle path is 0.40±0.07m, respectively. The figures show that our method is more accurate than the other two pure ZUPT-based methods.

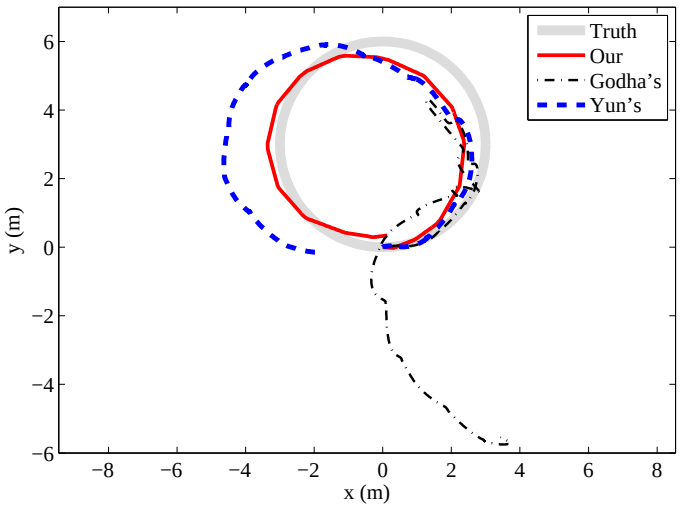

Fig. 6. One example of the estimated displacement results for walking in a circle with radius of 3m.

2) Long distance walking: both indoor and outdoor long distance walking experiments are conducted to further validate the feasibility of our method in long-term tests. The indoor experiment is carried out in a laboratory on campus. The walking path of the experiment is shown in Fig. 7, which totally covers about 132m in distance, with various obstacles and turns. Along the walking path, distinctive points with 1m distance are marked on the floor to guide the subjects to walk along the path. As shown in Fig. 7, the thick grey solid line in the plot represents the predefined path. From the start position which is the $(0, 0)$ point in the plot, the subject walks along the path, makes several turns and walks back to the starting position. The subject takes about 3 minutes to walk along it under normal walking speed. In Fig. 7, the thin solid line shows the estimated trajectory using the proposed method, the dash-dotted line is the results of Godha's method, while the dashed line illustrates the position estimation of Yun's method.

Similar to indoor walking, as shown in Fig. 8, the thick grey solid line represents the predefined path for the outdoor experiment. The total distance of the outdoor walking path is about 332m. From the starting position which is the original point in the plot, the subject walks along the path, makes several turns and walks back to the starting position. Under normal walking speed, it takes about 6 minutes for the subject to walk along the path. In Fig. 8, the thin solid line shows the estimated trajectory using our proposed method, the dash-dotted line follows Godha's method, and dashed line illustrates the position estimation by Yun's method. Both indoor and outdoor walking experiments are repeated 5 times, and the position errors of each test are shown in Table II. The average position errors over the 5 trials are also shown in the table. Based on our method, the averaged error for 3 minutes indoor walking is 4.31±1.77m, and for 6 minutes outdoor walking is 3.88±0.35m. The comparison results of the average position errors among the three methods indicates our method has achieved the highest accuracy in the long-term experiments.

TABLE I
ABSOLUTE INITIAL-FINAL POSITION ERROR FOR SHORT DISTANCE WALKING (UNIT: M)

Position error(%)	line			turn			circle		
	Our	Godha's	Yun's	Our	Godha's	Yun's	Our	Godha's	Yun's
1	0.21	2.19	1.52	0.40	1.20	0.44	0.34	5.52	1.00
2	0.63	1.86	2.93	0.50	0.64	1.00	0.37	6.53	1.77
3	0.64	1.63	2.10	0.55	0.54	1.08	0.36	6.15	0.89
4	0.44	1.23	1.39	0.36	0.64	0.46	0.52	7.82	0.65
5	0.28	1.70	0.87	0.44	0.89	0.39	0.41	3.97	1.28
mean±std	0.44±0.20	1.72±0.35	1.76±0.78	0.45±0.08	0.78±0.27	0.67±0.34	0.40±0.07	6.00±1.41	1.12±0.43

TABLE II
ABSOLUTE INITIAL-FINAL POSITION ERROR FOR LONG DISTANCE WALKING (UNIT: M)

Position error(%)	indoor			outdoor		
	Our	Godha's	Yun's	Our	Godha's	Yun's
1	5.35	14.68	9.03	4.16	22.01	8.13
2	2.11	7.18	8.94	3.39	16.17	12.48
3	2.69	18.70	14.90	3.87	21.98	12.08
4	5.93	19.95	14.80	4.25	21.45	10.79
5	5.48	13.56	15.09	3.72	17.70	8.33
mean±std	4.31±1.77	14.73±4.93	12.55±3.26	3.88±0.35	19.86±2.74	10.37±2.05

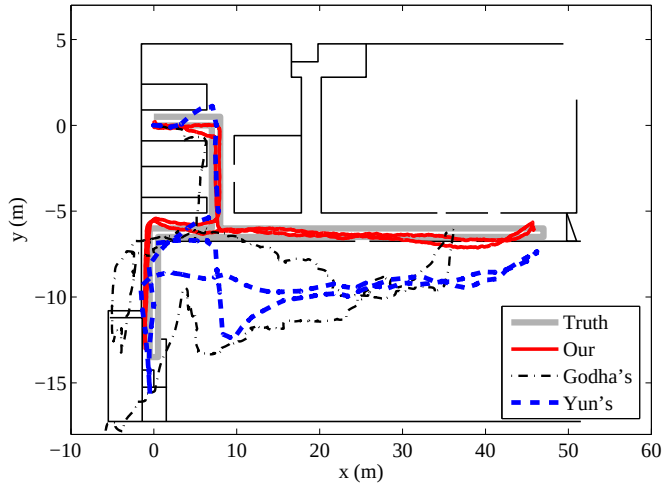

Fig. 7. One example of the displacement estimation for the indoor experiments.

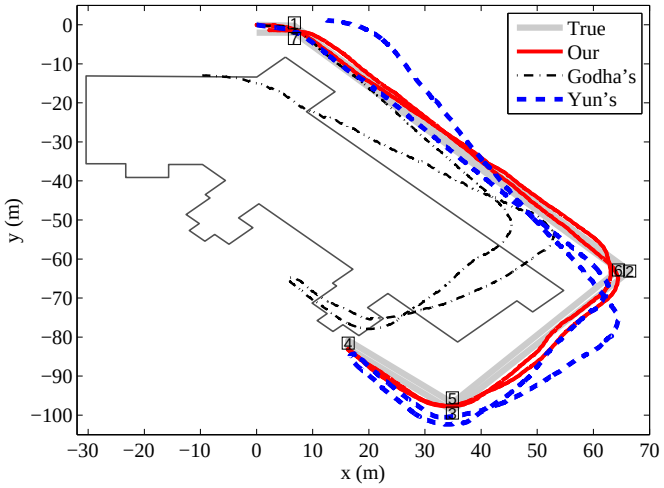

Fig. 8. One example of the displacement estimation for the outdoor experiments. The actual position of the 7 important points are marked by the square number plates.

C. Discussion

The performance of the proposed method has been extensively compared with those of the two pure ZUPT-based methods. As we can see from Table I and Table II, the proposed method has achieved the smallest position error compared with the other two methods. Compared with Godha's method, which simply resets the velocity to zero during the stance phase, Yun's method has improved the tracking accuracy. This is mainly because Yun's method not only applied ZUPT to the stance phase, but also applied a time-variant velocity drift error to revise the acceleration in the swing phase. However, in Yun's method, there was one stride delay in the position estimation, because it had to wait for the stride to be executed and then determined the drift error afterwards. Our method corrects the velocity using the different velocity control vectors in the stance phase or swing phase, without the introduction of the one-stride delay. Based on the results shown in Figs. 4–8, the integration of ZUPT with stride counting can significantly improve the tracking performance compared with the pure ZUPT-based methods. This is mainly due to the extracted average stride velocity and the position from stride counting, which can be used to further compensate for the acceleration double integration and thus improve the estimation accuracy. We also believe that with the tolerance of one stride delay, the tracking accuracy could be further improved by using the velocity of current stride as the control vector.

In our experiments, we use the position difference between the starting and final points to evaluate the performance of the proposed pedestrian tracking algorithm. Although it is commonly recognized in the assessment of the pedestrian tracking accuracy [9], [12], [16], the tracking performance

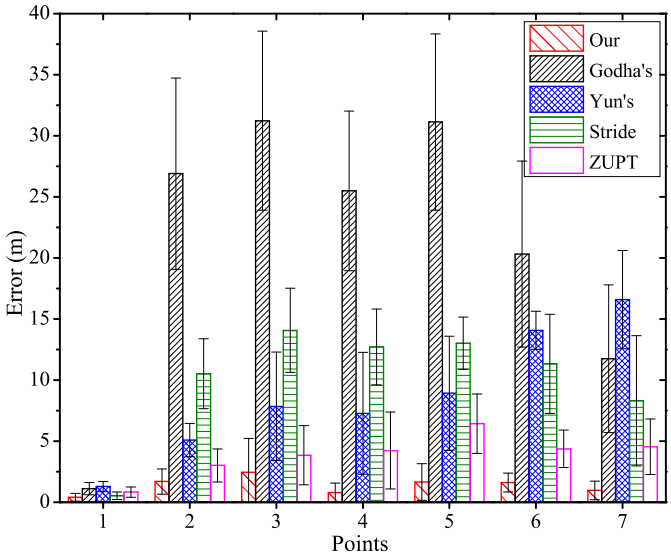

Fig. 9. The distance errors between the estimated position and actual position of the 7 important points.

may not be fully exploited by this method since it ignores the possible deviation of the other points from the walking path. Therefore, more points are extracted from the walking path for the performance evaluation. One possible way is to choose the critical turning points from the path of the ground truth. The corresponding turning points will be found manually from the position estimates provided by the three different methods. Then the position differences between these turning points can be calculated for performance comparison. Take the outdoor long-term walking as an example, except the starting and final points, 7 more points can be used for evaluation, which are marked by the square number plates in Fig. 8. The average distance errors and standard deviations between the estimated position and actual position of the 7 points from the 5 trials are shown in Fig. 9. To further illustrate how the stride information can be used to improve estimation accuracy of the ZUPT-based methods, the results of the pure stride-based method are also shown in the figure. It is evident that integration of the ZUPT-based method with stride-based method can achieve better results than applying any of the methods alone.

When stride is mis-detected/false-detected, or errors exist in the estimated stride length or heading direction, the pseudo measurement from stride counting should be regarded as invalid by setting the threshold λ_p. During our experiments, all the strides could be accurately detected, but the estimated stride length or heading direction had significant errors under some certain situations, like turning, activities switching (from standing still to walking or from walking to standing still) or even walking on the spot. Take the 180^o turn or sharp turn for example, the subjects normally did the turning at the same spot with little displacement change. In such case, the inaccurate pseudo measurement should be ignored, which was achieved via the threshold λ_p; the double integration could then take the leading role in position estimation to reduce the error in the pedestrian's location estimation. To further illustrate the behavior of the ZUPT method with/without intervention of the pseudo measurement model, different values of λ_p have been chosen to compare the displacement estimation performances. The pure stride-based method in Fig. 9 can be taken as the estimation results when $\lambda_p = \infty$, while the ZUPT method without any pseudo measurements intervention can be considered as the estimation results when $\lambda_p = 0$. It is evident that the displacement estimation performance is slightly better than the that of Yun's method when $\lambda_p = 0$, but not as good as our final results. Although the both of pure stride-based method and the ZUPT method without any pseudo measurements intervention work poorly, the integration of these two method can act as the best one. The possible explanation is that though the stride method is not performing good for turns and activity transitions or other situations, it outperforms double integration method in the rest of conditions. Therefore, by integrating of these two methods together, we have obtained best results.

IV. Conclusion and Future Work

In this paper, a novel pedestrian navigation method using a sole foot-mounted sensor module has been proposed, which integrates the ZUPT-based method with the stride-based method under the framework of an AKF. In order to compensate for the velocity drift, a velocity control variable has been designed in the process model, which has been set to the average velocity derived from stride information in the swing phases or zero in the stance phases. Stride-based position estimates are also derived as the pseudo-measurements to further improve tracking accuracy. The impressive experimental results have demonstrated that our proposed method can accurately track the positions of pedestrians in both indoor and outdoor environments.

The proposed method is only evaluated for normal walking experiments on level ground. Our future work will focus on further extending our method for other walking patterns, like backwards walking, sideways walking and stair climbing.

References

[1] E. Foxlin, "Pedestrian tracking with shoe-mounted inertial sensors," *Computer Graphics and Applications, IEEE*, vol. 25, no. 6, pp. 38–46, 2005.
[2] R. Ivanov, "Real-time GPS track simplification algorithm for outdoor navigation of visually impaired," *Journal of Network and Computer Applications*, vol. 35, no. 5, pp. 1559–1567, 2012.
[3] N. Fallah, I. Apostolopoulos, K. Bekris, and E. Folmer, "Indoor human navigation systems: A survey," *Interacting with Computers*, vol. 25, no. 1, pp. 21–33, 2013.
[4] Xsens MTx. [Online]. Available: http://www.xsens.com
[5] Microstrain 3DM. [Online]. Available: http://www.microstrain.com
[6] P. Groves, *Principles of GNSS, Inertial and Multisensor Integrated Navigation Systems*. Boston, London: Artech House, Inc, 2008.
[7] I. Skog, P. Handel, J. Nilsson, and J. Rantakokko, "Zero-velocity detection - an algorithm evaluation," *IEEE Trans. Biomed. Eng.*, vol. 57, no. 11, pp. 2657–2666, 2010.
[8] L. Ojeda and J. Borenstein, "Non-GPS navigation for security personnel and first responders," *J. Navigation*, vol. 60, no. 3, pp. 391–407, 2007.
[9] O. Bebek, M. Suster, S. Rajgopal, M. Fu, X. Huang, M. Cavusoglu, D. Young, M. Mehregany, A. van den Bogert, and C. Mastrangelo, "Personal navigation via high-resolution gait-corrected inertial measurement units," *IEEE T. Instrum. Meas.*, vol. 59, no. 11, pp. 3018–3027, 2010.
[10] E. Foxlin, "Pedestrian tracking with shoe-mounted inertial sensors," *IEEE Comput. Graph.*, vol. 25, no. 6, pp. 38–46, 2005.

[11] S. Godha and G. Lachapelle, "Foot mounted inertial system for pedestrian navigation," *Meas. Sci. Technol.*, vol. 19, no. 7, pp. 075 202:1–9, 2008.

[12] X. Yun, J. Calusdian, E. Bachmann, and R. McGhee, "Estimation of human foot motion during normal walking using inertial and magnetic sensor measurements," *IEEE T. Instrum. Meas.*, vol. 61, no. 7, pp. 2059–2072, 2012.

[13] C. Fischer, K. Muthukrishnan, M. Hazas, and H. Gellersen, "Ultrasound-aided pedestrian dead reckoning for indoor navigation," in *Proc. 1st ACM int. workshop MELT*, San Francisco, CA, USA, Sep. 2008, pp. 31–36.

[14] J. Hol, F. Dijkstra, H. Luinge, T. Schon, and B. Enschede, "Tightly coupled UWB / IMU pose estimation," in *Proc. IEEE Int. Conf. UWB*, Vancouver, BC, Sep. 2009, pp. 668–692.

[15] J. Corrales, F. Candelas, and F. Torres, "Hybrid tracking of human operators using IMU/UWB data fusion by a Kalman filter," in *Proc. 3rd ACM/IEEE int. conf. HRI*, Amsterdam, The Netherlands, Mar. 2008, pp. 193–200.

[16] A. Ruiz, F. Granja, J. Honorato, and J. Rosas, "Accurate pedestrian indoor navigation by tightly coupling foot-mounted IMU and RFID measurements," *IEEE Trans. Instrum. Meas.*, vol. 61, no. 1, pp. 178–189, 2012.

[17] Widyawana, G. Pirkl, D. Munaretto, C. Fischer, C. An, P. Lukowicz, M. Klepal, A. Timm-Giel, J. Widmer, D. Pesch, and H. Gellersen, "Virtual lifeline: multimodal sensor data fusion for robust navigation in unknown environments," *Pervasive and Mobile Computing*, vol. 8, no. 3, pp. 388–401, 2012.

[18] C. Toth, D. A. Grejner-Brzezinska, and S. Moafipoor, "Pedestrian tracking and navigation using neural networks and fuzzy logic," in *Intelligent Signal Processing, 2007. WISP 2007. IEEE International Symposium on*. IEEE, 2007, pp. 1–6.

[19] Y. Jin, H.-S. Toh, W.-S. Soh, and W.-C. Wong, "A robust dead-reckoning pedestrian tracking system with low cost sensors," in *Pervasive Computing and Communications (PerCom), 2011 IEEE International Conference on*. IEEE, 2011, pp. 222–230.

[20] X. Meng, Z. Zhang, S. Sun, J. Wu, and W.Wong, "Biomechanical model-based displacement estimation in micro-sensor motion capture," *Meas. Sci. Technol.*, vol. 23, no. 5, pp. 055 101:1–11, 2012.

[21] J. Kuipers, *Quaternions and Rotation Sequences: a primer with applications to orbits, aerospace, and virtual reality*. Princeton, NJ: Princeton Univ. Press, 1999.

[22] D. Choukroun, I. Bar-Itzhack, and Y. Oshman, "Novel quaternion Kalman filter," *IEEE Trans. Aero. Elec. Sys.*, vol. 42, no. 1, pp. 174–190, 2006.

[23] S. Sun, X. Meng, L. Ji, J. Wu, and W. Wong, "Adaptive sensor data fusion in motion capture," in *Proc. 13th Int. Conf. Info. Fusion*, Edinburgh, UK, Jul. 2010, pp. 1–8.

[24] D. Alvarez, R. Gonzaléz, A. López, and J. Alvarez, "Comparison of step length estimators from wearable accelerometer devices," in *Proc. IEEE EMBS*, Amsterdam, The Netherlands, Aug. 2006, pp. 5964–5967.

[25] E. Wan and R. V. D. Merwe, "The Unscented Kalman filter for nonlinear estimation," in *Proc. IEEE AS-SPCC*, Lake Louise, Alta., Canada, Oct. 2000, pp. 153–158.

[26] Analog Devices ADIS16405. [Online]. Available: http://www.analog.com/en/memssensors/mems-inertial-sensors/adis16405/products/product.html/

Xiaoli Meng received the B.E. degree in communication engineering from Tianjin University, China, in 2007, and the Ph.D. degree from the Sensor Network and Application Research Center, Graduate University, Chinese Academy of Sciences, Beijing, China, in 2012. She is currently a Research fellow in the Department of bioengineering, Nation University of Singapore. Her research interests include human motion tracking, gait analysis, and rehabilitation robotics.

Zhi-Qiang Zhang received the B.E. degree in computer science and technology from School of Electrical Information and Engineering, Tianjian University, China, in 2005, and the Ph.D. degree from the Sensor Network and Application Research Center, Graduate University, Chinese Academy of Sciences, Beijing, China, in 2010. He is currently a Research Associate in the Department of Computing, Imperial College, London. His research interests include Body Sensor Network, Information Fusion, Machine Learning and Targets Tracking..

Jian-Kang Wu received the B.Sc. degree from the University of Science and Technology of China (UTSC), China, in 1970, and the Ph.D. degree from Tokyo University, Tokyo, Japan, in 1992. He is currently a professor in the Graduate University, Chinese Academy of Sciences, Beijing, China and directing the Sensor Networks and Application Research Center. Prior to the current position, he was the Principal Scientist and Department Manager of New Initiatives Department at Institute for Infocomm Research (I2R), Singapore. He created new research initiatives in the areas of NeuroInformatics, PhysioInformatics, and embedded sensor network systems in I2R, and led a series of large international collaborative projects in KRDL and ISS. He is an author of 18 patents, more than 100 papers, and 5 books. He received nine distinguished awards from the nation and Chinese Academy of Sciences.

Wai-Choong Wong received the B.Sc. Hons. and Ph.D. degrees in Electronic and Electrical Engineering both from Loughborough University, UK, in 1976 and 1980, respectively. He is currently a Professor in the Department of Electrical and Computer Engineering, National University of Singapore (NUS), Singapore. He is also holding the position of Deputy Director (Strategic Development) at the Interactive and Digital Media Institute in NUS. He was previously the Executive Director of the Institute for Infocomm Research (I2R) from Nov 2002 to Nov 2006. Since joining NUS in 1983, he served in various positions at the department, faculty, and university levels, including the Head of the Department of Electrical and Computer Engineering from Jan 2008 to Oct 2009, Director of the NUS Computer Center from Jul 2000 to Nov 2002, and Director of the Centre for Instructional Technology from Jan 1998 to Jun 2000. Prior to joining NUS in 1983, he was a Member of Technical Staff at ATT Bell Laboratories, Crawford Hill Lab, NJ, USA, from 1980 to 1983. He has more than 200 publications and four patents in these areas. He is a co-author of the book "Source-Matched Mobile Communications." His research interests include wireless networks and systems, multimedia networks, and source matched transmission techniques. Dr. Wong received the IEEE Marconi Premium Award, in 1989, NUS Teaching Award, in 1989, IEEE Millennium Award, in 2000, the e-nnovator Awards, in 2000, Open Category, and Best Paper Award at the IEEE International Conference on Multimedia and Expo, in 2006.

Haoyong Yu is an Assistant Professor of Department of Bioengineering at NUS. He received his PhD in Mechanical Engineering from MIT in 2002. His PhD research at MIT was to develop smart personal mobility aids and health monitoring systems for the elderly, with his main contribution in the areas of omni-directional mobility design and adaptive shared control for human machine interaction. He then worked in DSO National Laboratories of Singapore as a Principal Member of Technical Staff. His research areas in DSO included exoskeleton and humanoid robots as well as intelligent ground and aerial robots. Dr. Yu joined Department of Bioengineering of NUS in September 2010. His current research focus is on robotics for neurorehabilitation, especially on using exoskeleton systems and smart mobility aids for patients with stroke and Parkinson's Diseases. His is collaborating with NUHS, SGH, DSO, MIT, UPMC of France, and Maebashi Institute of Technology of Japan for his research.